AMERICAN UNIVERSITY OF BEIRUT

ESTABLISHING A NOVEL IN VITRO MODEL OF PROSTATE CANCER STARTING FROM STEM/PROGENITOR CELLS

by

LAYAL HASAN HAMDAR

A thesis
submitted in partial fulfillment of the requirements
for the degree of Master of Science
to the Department of Anatomy, Cell Biology, and Physiology
of the Faculty of Medicine
at the American University of Beirut

Beirut, Lebanon
April 2015

AMERICAN UNIVERSITY OF BEIRUT

ESTABLISHING A NOVEL IN VITRO MODEL OF PROSTATE CANCER STARTING FROM STEM/PROGENITOR CELLS

by

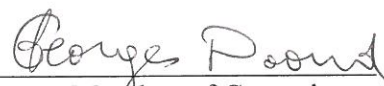### Layal Hasan Hamdar
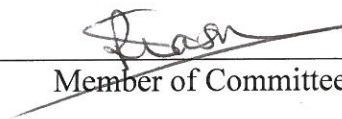
Approved by:

_____   Advisor
Wassim Abou-Kheir, Assistant Professor
Departments of Anatomy, Cell Biology & Physiology

_____   Co-Advisor
Assaad A. Eid, Assistant Professor
Departments of Anatomy, Cell Biology & Physiology

_____   Member of Committee
Georges Daoud, Assistant Professor
Departments of Anatomy, Cell Biology & Physiology

_____   Member of Committee
Rihab Nasr, Associate Professor
Departments of Anatomy, Cell Biology & Physiology

Date of thesis defense: April 28, 2015

AMERICAN UNIVERSITY OF BEIRUT

THESIS, DISSERTATION, PROJECT RELEASE FORM

HAMDAR LAYAL HASAN

Student Name: _____

                Last   First   Middle

⬭ Master's Thesis   ⬭ Master's Project   ⬭ Doctoral   Dissertation

☐   I authorize the American University of Beirut to: (a) reproduce hard or electronic copies of my thesis, dissertation, or project; (b) include such copies in the archives and digital repositories of the University; and (c) make freely available such copies to third parties for research or educational purposes.

☐   I authorize the American University of Beirut, **three years after the date of submitting my thesis, dissertation, or project,** to: (a) reproduce hard or electronic copies of it; (b) include such copies in the archives and digital repositories of the University; and (c) make freely available such copies to third parties for research or educational purposes.

_____

Signature   Date

ACKNOWLEDGMENTS

First and Foremost, I am grateful to Allah ,most gracious most merciful ,for all of his blessings .Thank you God for keeping me and my family always safe and healthy.

I would like to start by thanking the Department of Anatomy, Cell biology and Physiology and Chairperson Dr. Nayef Saade for taking me in as a graduate student during these years.

My deepest respect and the utmost appreciation goes to my advisor and mentor Dr. Wassim Abou-Kheir. Thank you Dr. Wassim for your endless support and patience. You have taught me so much throughout these years. You have taught me science and you have taught me life. I am forever grateful.

Dr Assaad Eid, my co-advisor, words cannot express how thankful I am for everything you did for me. Thank you for your support and encouragement since day one. Thank you for always keeping your door open for me and all your students. It is your constant care that makes you a great graduate advisor.

I would like to take this chance to thank my committee members Dr. Georges Daoud and Dr. Rihab Nasr. Thank you for taking the time to read my thesis and give me your feedback.

Alissar, my dearest, I could not have done any of this without you. You are not just my labmate, you are a close friend. Without your help and time, none of this would have been possible. We have been through so much together and I enjoyed every minute with you and the girls. Cheers to many more happy moments and memories.

A special thank you to all my labmates and friends: Ola, Rabieh, Tarek, Carla, Sami, Wafaa, Farah, and Hisham. Thank you for all the fun times. You guys are the best support system any one could ask for.

I would also like to thank my girls Rebecca, Fatima and Ghina for always being there for me. Alissar you are part of this too. Thank you for all the laughs and the memories. Thank you for always keeping me in check.

I want to take a moment and thank my best friend , my rock ,my guardian angel, and the person dearest to my heart. Thank you Mohammad Kanso for your never ending support. Thank you for always pushing me forward. Thank you for always keeping me grounded. Most of all, thank you for always keeping me close to God. I am truly blessed.

I would also like to thank my girlfriends: Farah, Nour, Maha, Al-Zahraa, Sirine, Ranim and Nadine. Thank you for being there for me through it all. Thank you for listening to my nagging about reviews, cells, and mice. I love you all.

Last but definitely not least, my beloved family. Thank you mom and dad. Thank you for the world. Thank you for dedicating your life so that my siblings and I could have a great one. Thank you for all the sacrifices you make and the time you spend watching over us. No words are enough. I love you both.

Rawan, Mohammad and Kareem I love you guys. Although we may fight; all brothers and sisters do. You remain my best friends through everything.

I ask the Lord to keep everyone safe and healthy.

God Bless and God Speed.

AN ABSTRACT OF THE THESIS OF

Layal Hasan Hamdar   for   Master of Science
                                    Major: Human Morphology

Title: Establishing A Novel In Vitro Model Of Prostate Cancer Starting From Stem/Progenitor Cells

Cell lines representing the progression of prostate cancer from an androgen-dependent to an androgen-independent state are scarce. Previously, we have established and characterized a new murine prostate luminal epithelial cell line (PLum), with *Pten/TP53* deletions, derived from a prostate epithelial stem/progenitor-enriched cell population. The deprivation of androgens from established PLum-orthotopic tumors resulted in tumor regression and eventually castration-resistant growth. Cells derived from orthotopic tumors have been isolated to develop androgen-dependent versus androgen-independent model. In this study, several experiments were conducted to establish and investigate the functional differences of the newly isolated androgen-dependent (PLum-AD) and androgen-independent (PLum-AI) murine prostate cancer cell lines. Unlike PLum-AD cells that grew in serum-free medium, PLum-AI cells grew better in 5% FBS-containing medium. Both cell lines remained faithful in morphology to their in vivo source, where PLum-AD showed a typical epithelial morphology (in vivo source: adenocarcinoma) and PLum-AI showed an epithelial-to-mesenchymal morphology (in vivo source: sarcomatoid carcinoma). Furthermore, upon immunofluorescent analysis, PLum-AD cell expressed mostly prostate epithelial markers while PLum-AI cells expressed mesenchymal cell markers. In addition, QRT-PCR and Western blot analysis confirmed the epithelial and mesenchymal morphology of PLum-AD and PLum-AI respectively. To assess for the presence of stem/progenitor cell population, the cells were subjected to sphere-formation assay. Both cell lines had the capacity to form spheres, where PLum-AD cells formed regular-shaped spheres and PLum-AI cells formed mostly large stellate shaped spheres consistent with their mesenchymal-like nature. Interestingly, and despite a lower level in PLum-AI, both cell lines showed expression of AR at the mRNA and protein levels. Although both cell lines showed tumorigenic abilities, PLum-AI was significantly more aggressive in terms of tumor volume and mice survival compared to PLum-AD cells. These data suggest that the newly isolated cell lines represent a new in vitro model of androgen-dependent and –independent prostate cancer where they recapitulate the progression of the disease to a more invasive phenotype upon androgen deprivation.

CONTENTS

FIGURES

ABBREVIATIONS

ADT	Androgen Deprovation Therapy
AIPC	Androgen-Independent Prostate Cancer
AMPK	Adenosine-Monophosphate Protein Kinase
AR	Androgen Receptor
BPH	Benign Prostatic Hyperplasia
CK	Cytokeratin
CRPC	Castration-Resistant Prostate Cancer
DHT	Dihydrotestosterone
EMT	Epithelial Mesenchymal Transformation
GnRH	Gonadotropin-Realeasing Hormone
LHRH	Luteinizing Hormone Releasing Hormone
NOD-SCID	Nonobese Diabetic-Severe Combined Immunodeficiency
PC	Prostate Cancer
PIN	Prostate Intraepithelial neoplasia
PLum-AD	Prostate luminal-Androgen Dependent
PLum-AI	Prostate luminal-Androgen Independent
PSA	Prostate Specific Antigen

INTRODUCTION

A. Overview

1. The Prostate Gland: Structure and Function

The prostate is a small walnut-shaped tubulo-alveolar exocrine gland of the male reproductive system. It is located in the pelvis, surrounding the urethra just below the urinary bladder. The primary function of the prostate gland is to secrete a milky alkaline fluid that comprises 30% of the volume of semen. This fluid prolongs sperm life span and improves its motility. The prostate is divided into three distinct zones: The transitional, central and peripheral zones (Fig. 1). The transitional zone makes up 5% of the prostate gland. Only 10-20 % of prostate cancers originate in this zone. It surrounds the proximal urethra and grows throughout a person's life. The central zone makes up 25% of the prostate gland and surrounds the ejaculatory ducts. Only 3% of prostate cancers originate in this zone. The peripheral zone makes up 70% of the prostate gland and surrounds the distal urethra.70-80% of prostate cancers originate in this zone (Myers, 2000).

2. Epithelial Components of the Prostate Gland

The prostate is made of three epithelial cell types: basal cells, luminal cells and neuroendocrine cells (Fig. 1). Basal cells form the proliferative layer of the prostate (Bonkhoff, 1994). This layer consists of cells mainly expressing cytokeratins CK5 and CK14. However, the luminal cells make up the secretory layer, and is mainly characterized by expressing cytokeratins CK 8 and CK 18 (long, 2005). The neuroendocrine cells are located between the basal and the luminal layer. Those cells have a role in normal prostate gland development. Although prostate adenocarcinomas are characterized by a luminal phenotype expressing

androgen receptors (AR) (Abou kheir, 2011), it has been hypothesized that the basal layer of the prostate has a stem-like population that may be responsible for the development of the three epithelial cell types of the prostate (Isaacs, 1989).
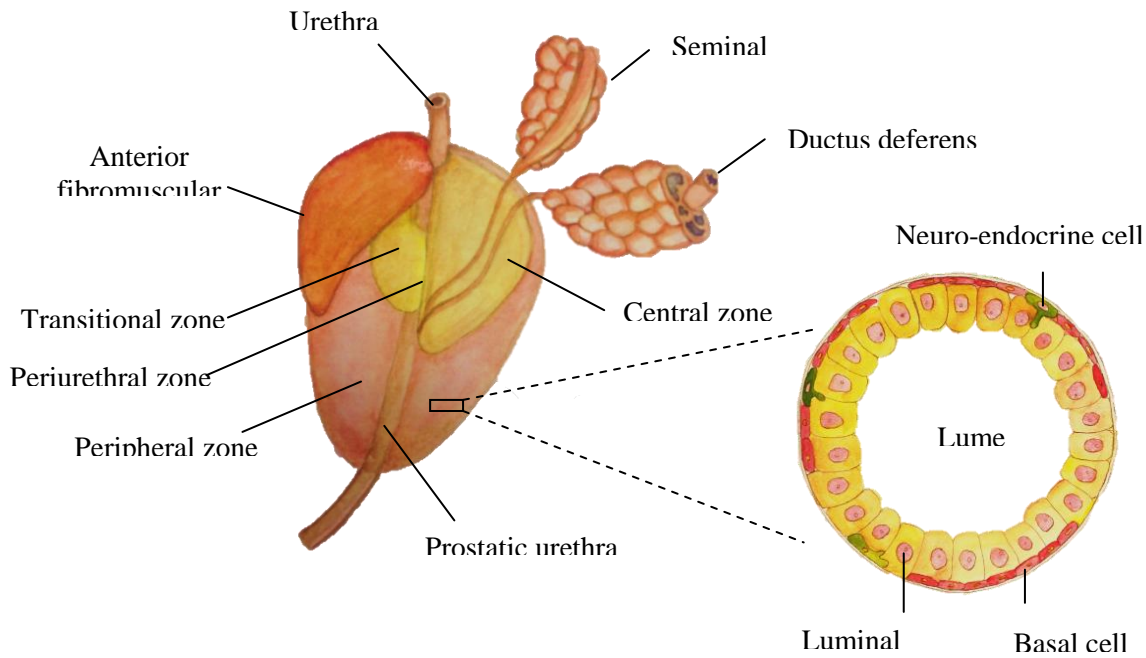
Figure 1 . The prostate gland and its cellular components.
Schematic representation showing the different zones that comprise the prostate gland and its cellular composition.
Bahri ,D.K (2013) *Sea Cucumber Extracts Inhibit the Proliferation of Prostate Cancer cells and Cancer Stem-like cells*.M.Sc Thesis.American University of Beirut: Lebanon

3. Prostate Specific Antigen

Prostate specific antigen (PSA) is a protein secreted by the epithelial (luminal) cells of the prostate gland. PSA has a role in semen liquefaction, as well as in dissolving cervical mucus allowing easier sperm access into the uterus (Balk, 2002). PSA is found in small quantities in the serum of healthy men. An elevation in the serum levels of PSA may indicate a problem in the prostate gland (hypertrophy or hyperplasia). PSA levels are not only elevated in prostate cancer,

but also in conditions such as prostatitis, Benign prostatic hyperplasia (BPH) and other prostate disorders (Herschman, 1997).

B. Benign Prostatic Hyperplasia

Benign Prostatic Hyperplasia (BPH) is a very common non-malignant condition in older men characterized by the enlargement of the prostate gland (McNicholas, 2011). This enlargement is usually associated with an increase in serum PSA. Studies have shown that BPH may be the result of high estrogen levels that are produced in men as they age. Although many cases of prostate cancer are found in patients who already have BPH, BPH does not cause prostate cancer (Lalani et al, 1997). Unlike prostate cancer, BPH originates in the transitional zone of the prostate gland and is histologically characterized by a basal cell layer (Bonkhoff, 1996). BPH and Prostate Cancer(PC) have similar symptoms. Since the prostate surrounds the urethra, BPH may cause: Hesitancy, frequent urination, nocturia, hematouria, bladder infection, and urinary tube blockage in its advanced stages. Similar to prostate cancer, ADT may be used to treat cases of PBH. Other treatments may include surgery or other minimally invasive treatments.

C. Prostatic Intraepithelial Neoplasia

Prostatic Intraepithelial Neoplasia (PIN) is the premalignant condition preceding prostate cancer (Bostwick, 2000). It is usually asymptomatic and often considered as a form of localized cancer. It is characterized by the abnormal interruption of the basal cell layer of the prostatic ducts and acini (Gonzalez, 2012). PIN is a significant risk factor for prostate adenocarcinoma where in 85% of the cases, PIN and prostate cancer coexist (Bostwick, 2000).

D. Development and Progression of Prostate Cancer

Prostate cancer is one of the most commonly diagnosed slow growing cancers among men worldwide. Cancer in the prostate gland may cause no symptoms during its early stages. Since 70-80% of prostate tumors develop in the peripheral zone which is distal to the urethra, urinary problems may not occur until the disease progresses (Ahmed et al, 1997) .As it advances into later stages, symptoms like pelvic pain, painful urination, and hematouria may start to occur. Prostate cancer is epithelial in nature (long, 2005). Since most cells in the prostate are glandular, the majority of prostate tumors are adenocarcinomas (long, 2005). Researchers agree that PIN is a precursor for Prostate cancer (Demarzo et al, 2003). PIN is characterized by the decrease in the epithelial basal cells and a noticeable increase in the luminal cells (chen et al, 2010). When the disease starts progressing, the epithelium loses most of its basal cells and is mostly of a luminal phenotype. This is the stage characterized as prostate cancer or prostate adenocarcinoma. The dissemination of these luminal cells to organs outside the prostate marks the beginning of metastatic prostate cancer (Fig. 2). Organs that may be a target of prostate cancer metastasis are bones, lymph nodes, liver, lungs and dura mater.
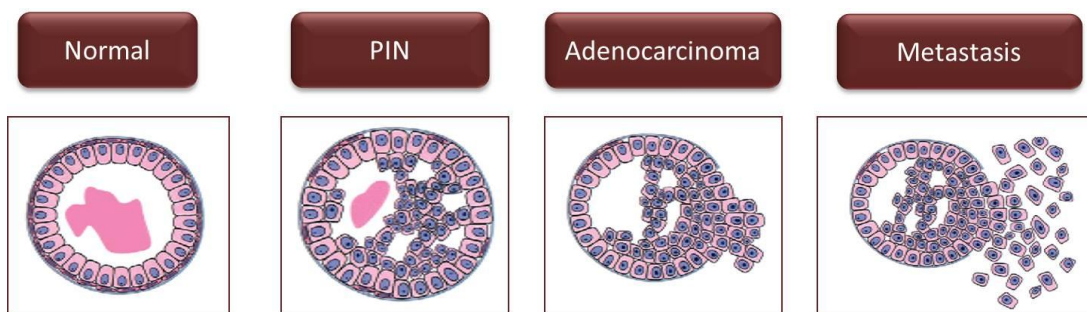
Figure 2. Stages and Advancement of Prostate Cancer. Normal prostate epithelium consists of basal, luminal and Neuroendocrine cells. As PIN develops, the luminal layer starts proliferating and the basal layer starts diminishing. This advances into Prostate carcinoma where the gland is mostly of a luminal phenotype. Metastasis, the malignant stage, is the spread of luminal cells outside the prostate into adjacent organs. Adapted and modified from Shen and Shen 2010.

E .Response to Treatment

Cases of prostate cancer, where the tumor is confined to the prostate gland, respond very well to treatment and are usually cured. Treatment regimens for these cases may include the surgical removal of the prostate (prostatectomy), chemotherapy, radiotherapy, or a combination of several of the above regimens (Hong et al, 2009). Unfortunately, patients with late stage prostate cancer respond poorly to treatment. Hormone therapy or androgen deprivation therapy (ADT) is usually the treatment of choice for patients suffering from aggressive prostate cancer. Prostate Cancer, just like the normal prostate gland, depends on androgens to grow. For this reason, ADT may result initially in tumor shrinkage (Perlmutter et al, 2007). The main purpose of ADT is to reduce the levels of testosterone and dihydrotestosterone (DHT) or stop their effect on prostate cancer cells. This could be done surgically by removing the testicles (surgical castration) or chemically by injecting Luteinizing Hormone releasing Hormone (LHRH) into the patient's body (chemical castration). However, many patients will experience recurrent Castrate-Resistant Prostate Cancer (CRPC) or Androgen Independent Prostate Cancer (AIPC) (Dilorenzo et al, 2010). CRPC is considered the malignant stage of the disease. This will result in cancer metastasis into the bones, brain and lymph nodes eventually leading to patient death. Multiple mechanisms seem to be involved in the development of CRPC, however strong evidence show that one mechanism might involve the presence of prostate cancer progenitor cells that lack androgen receptors (Abou kheir et al, 2011).

Some treatments of prostate cancer include the oral non-steroidal anti-androgen Bicalutamide or Casodex. This drug is used for the treatment of prostate cancer, usually at primary stages. It may be used on its own, or combined with a GnRH agonist in advanced cases of CRPC (Klotz et al, 2006, Wellington et al, 2006). Bicalutamide acts by binding to androgen

receptor (AR) thus preventing its activation and accelerating its degradation (Furr Bj et al, 1996). Enzalutamide is another androgen receptor antagonist that is used to treat CRPC (Shalken, 2015). Docetaxel is another drug used for the treatment of advanced prostate cancer. It is a chemotherapeutic drug that intervenes in cell division and improves life expectancy (Shelley et al, 2006). Degarelix is used as hormone therapy to treat CRPC. It works by inhibiting GnRH binding to their receptors and thus inhibiting the production of testosterone (Princivalle et al, 2007). Another treatment for metastatic CRPC, is the drug Abiraterone that is used in combination with the immunosuppressant Prednisone. Abiraterone works by inhibiting the enzyme 17 α-hydroxylase which is responsible for the conversion of androgen precursors into testosterone thereby decreasing serum levels of testosterone (Attard et al, 2005). Many other drugs are used in the treatment of advanced prostate cancer or CRPC. Understanding the biology of prostate cancer and the cellular origins and progression of CRPC is a major goal of prostate cancer research.

F. Androgen Effect on the Progression of Prostate Cancer

Androgens are crucial for the proper development of the prostate gland. Androgen deprivation causes prostate atrophy. Androgens act on stromal and epithelial cells of the prostate, therefore upon androgen deprivation epithelial cells die (Montalvo, 2000). It is widely known that prostate cancer cells require androgens to grow and develop. This is usually during the early stages of the disease. Androgen regulation is achieved through androgen receptors (AR) signaling pathway (Schalken et al, 2015). AR plays a role in all phases of prostate cancer from its initiation to its metastasis and spread (Schalken et al, 2015). In prostate epithelial and stromal cells, testosterone is converted into the active form DHT by 5-α reductase (Heinlein et al, 2004).

Testosterone or DHT binds to the ligand binding domain of AR, causing a conformational change and activation of the receptor leading to the translocation of the AR from the cytosol to the nucleus. In the nucleus, the AR binds to androgen response elements of DNA, recruiting co-factors that regulate transcription of target genes such as PSA (Heinlein et al, 2004 ; Knudsen et al, 2011). As the cancer progresses, cells no longer respond to androgens entering the androgen-independent or the CRPC phase of the disease which is the malignant and lethal stage of the disease (Shalken et al, 2015).

G. Prostate Cancer Cell Models

What is known concerning the molecular physiological basis of primary prostate cancer and androgen-independent metastatic prostate cancer is drawn mainly from clinical samples and from the 3 human prostate cancer cell lines (LnCaP, DU145, and PC3) (Kaighn, M. E et al, 1979; Stone, K. R et al, 1978; Horoszewicz, J. S et al, 1980). With respect to clinical samples, most samples are prostatectomy samples of primary PC, which differ in their degree of invasiveness. It is quite rare to obtain resected specimens of metastatic lesions, as surgery is generally aborted if growth outside the prostate is observed, and androgen-deprivation therapy is begun. Human PC samples have been exceedingly difficult to establish as lines in culture, and the 3 lines referred to above were established from metastases (Kaighn, M. E et al 1979; Stone, K. R et al, 1978; Horoszewicz, J. S et al, 1980). PC-3 is an androgen-independent cell line derived from bone metastasis of prostate cancer. PC-3 has a very high metastatic ability (Pulukuri et al, 2005). DU145 is an androgen-independent cell line derived from brain metastasis (Stone et al, 1978). Compared to PC-3, DU145 is of moderate metastatic potential (Pulukuri et al, 2005). Neither PC-3 nor DU145 express PSA. LnCaP is an androgen-dependent cell line of

low metastatic potential. It is derived from lymph node prostate cancer metastasis. LnCaP expresses both PSA and AR (Horoszewicz, J. S et al, 1980). Although a few more lines do exist, they either require maintenance by passaging in animals or grow so slowly as to not be useful for mechanism-based investigations.

Cell lines representing the progression of prostate cancer from an androgen-dependent to an androgen-independent state are scarce. It is becoming apparent that establishing new prostate cancer cell lines representing the androgen-dependent and independent stages of the disease would be vital in deciphering the mechanistic changes that lead to development of CRPC stage.

H. Aim of the Study

Previously, we have established and characterized a new prostate luminal epithelial cell line (PLum), with *Pten/TP53* deletions, derived from a prostate epithelial stem/progenitor-enriched cell population (Abou-Kheir W et al, 2011). The deprivation of androgens from established PLum-orthotopic tumors resulted in tumor regression and eventually castration-resistant growth. Cells derived from orthotopic tumors have been isolated to develop androgen-dependent versus androgen-independent model.

In this study, we aim to

1- Establish and investigate the functional differences of the newly isolated androgen-dependent (PLum- AD) and androgen-independent (PLum-AI) murine prostate cancer cell lines.

2- Assess the tumorigenic potential of both PLum-AD and PLum-AI cells in different functional assays in vitro and in vivo.

3- Evaluate the stem/progenitor cell activity in PLum-AD and PLum-AI cells

8

4- Eventually, we hope to use this new cell model to understand the progression, at the molecular level, of prostate cancer from androgen-dependent to androgen-independent stage, and to use it as a tool for screening novel therapeutics.

MATERIALS AND METHODS

A. Cell Culture

PLum-AD and PLum-AI cells were plated in T75 cm2 flasks initially with serum-free prostate epithelial cell basal media, PrEGM. For an optimum growth of PLum-AI cells, 5% FBS was added to the media. The flasks were incubated at 37°C in a humidified incubator containing 5% CO2. The media over the cells was changed every other day. Upon reaching 70% confluency, cells were propagated using regular trypsinization methods. Bright field phase contrast images, using an inverted light microscope, were taken to assess for any changes in morphology.

B. Western Blot Analysis

Western Blot (WB) analysis was performed to study the protein expression levels of the genes examined by qRT-PCR. Protein samples were extracted in 2X sample buffer. Samples were loaded onto a 10% sodium dodecyl sulfate-polyacrylamide gel, subjected to electrophoresis, and transferred onto nitrocellulose membranes. The membranes were blocked with 5% skimmed milk in phosphate-buffered saline (PBS) containing 0.05% Tween-20 for 30 minutes at room temperature. Membranes were incubated with the specific primary antibodies overnight at 4°C. The primary antibodies used were as follow: Mouse monoclonal anti-CK8 and Rabbit polyclonal anti-CK14 (Covance), Rabbit monoclonal anti-AR (epitomics/abcam), Mouse monoclonal anti-Vimentin (abcam), Rabbit monoclonal anti-E-cadherin (Cell Signaling) and Mouse monoclonal anti-GAPDH (Novus Biologicals). The next day, membranes were washed, incubated with goat anti-mouse or goat anti-rabbit HRP-conjugated secondary antibodies (Santa Cruz), and then protein bands were visualized using enhanced chemiluminescence (ECL, Roche).

C. MTT/Cytotoxicity Assay

Anti-proliferative and cytotoxic effects of the different drugs used were measured *in vitro* via MTT ([3-(4, 5-dimethylthiazol-2-yl)-2, 5-diphenyltetrazolium bromide]) assays according to manufacturer's recommendation (Sigma). PLum-AD and PLum-AI cells were seeded in 100 μl complete medium in 96-well culture plates at a density of 3000 cells/ well. Cells were incubated overnight in the incubator and then treated in triplicates with various drug concentrations diluted in 100 μl complete media for 24, 48 and 72h. For each time point, 20 μl of 5 mg/ml MTT reagent, diluted in 1x PBS, was added to each well and incubated at 37°C for 4h. Finally, 100 μl of solubilization solution was added into each well to dissolve the formazan crystals. The reduced MTT optical density (OD) was measured at a wavelength of 595 nm using an ELISA reader (Multiskan Ex). The percentage of cell viability was presented as an OD ratio between the treated and untreated cells at the indicated concentrations. The different drugs used were Bicalutamide (10 um) and Metformin (1mM, 5mM, 10mM, and 50mM) (Sigma).

D. Immunofluorescence and morphological analysis for cells (2D)

Cells were seeded and adherent cells were fixed in 4% paraformaldehyde (PFA) in PBS for 10 min, followed by permeabilization with 0.5% Triton X-100 in PBS for 4 min. Non-specific sites were blocked by incubating them in a blocking buffer (0.1% BSA, 0.2% Triton X-100, 0.05% Tween-20, and 10% normal goat serum in PBS) for 30 min. Cells were then incubated overnight at 4°C with the specified antibodies in 2% BSA/PBS. The primary antibodies used were as follow: Mouse monoclonal anti-CK8 and Rabbit polyclonal anti-CK14 (Covance), Rabbit Polyclonal anti-Vimentin (Santa Cruz). Cells were washed three times with

PBS containing 0.1% Tween-20, incubated with Alexa-488 goat anti-mouse and Alexa-568 goat anti-rabbit conjugated IgG (Invitrogen) in 2% BSA for 30 min at room temperature. The anti-fade reagent Fluoro-gel II with DAPI (Electron Microscopy Sciences) was used for mounting. Fluorescent signals were captured using Zeiss LSM 710 confocal microscope and images were acquired and analyzed using the ZEN image software.

E. Sphere Formation Assay

In this study, both PLum-AD and PLum-AI cells were able to form spheroids in non-adherent culture, suggesting the presence of cancer stem-like cells within these cell lines. After counting the single cell suspension of prostate cancer cell lines, a concentration of 2,000 cells/ well of a 12-well plate were suspended in cold Matrigel^{TM}/ serum-free PrEGM media (1:1) in a total volume of 100 μl. Cells were seeded uniformly in a circular manner around the bottom rim of a well in a 12-well plate and allowed to solidify in the incubator at 37°C for 45 minutes, before 0.5 ml of PrEGM media was added gently in the middle of each well. Spheres were replenished with warm media as in the original seeding (with or without treatment) every two to three days. Spheres were counted after 10 days. To propagate spheres, the medium was aspirated and Matrigel^{TM} was digested with 0.5 ml Dispase solution (Invitrogen, 1 mg/ml, dissolved in PrEGM) for 60 minutes at 37°C. Spheres were collected, incubated in 1 ml warm Trypsin-EDTA at 37°C for 5 minutes. Trypsin was inhibited by FBS-conatining media and then spheres were passed through a series of needles with different gauges starting with 23, 25 and then 27-gauge syringe for 5 times each until single cell suspension is achieved. Cells were counted by a hemocytometer and re-seeded for further propagation as described earlier.

F. Immunofluorescence and morphological analysis for protospheres (3D)

Cells were grown in 6-well plates in Matrigel^TM-containing media as described before. Spheres were later collected in 1.5 ml Eppendorf tubes and fixed in 4% PFA at room temperature for 30 min. The PFA was aspirated gently and spheres were permeabilized with 0.5% Triton X-100 for 30 min at room temperature. After carefully aspirating the permeabilization solution, spheres were blocked using the sphere blocking buffer (0.1% BSA, 0.2% Triton X-100, 0.05% Tween-20, and 10% normal goat serum in PBS) for 2 hrs at room temperature. Spheres were incubated overnight with primary antibodies at 4°C. The primary antibodies were as follow: Rabbit Polyclonal anti-CK14 and mouse monoclonal anti-CK8 (Covance) and Rabbit polyclonal anti-beta3 tubulin (abcam). After gentle washing with PBS containing 0.1% Tween-20, spheres were incubated with Alexa-488 goat anti-mouse and Alexa-568 goat anti-rabbit conjugated IgG for 2 hrs at room temperature. For F-actin staining, spheres were incubated with rhodamine phalloidin (Invitrogen). The sphere pellet was washed and anti-fade reagent Fluorogel with DAPI was added, and then the spheres were mounted onto glass slides and covered with thin glass coverslips. Fluorescent signals were captured using Zeiss LSM 710 confocal microscope and images were acquired and analyzed using the ZEN image software.

G. Transwell Invasion Assay

For the invasion assay, 2.5×10^5 cells were seeded in a serum-free medium with or without treatment in the top chamber onto the Matrigel^TM-coated membrane (24-well insert; pore size, 8 µm; Falcon), and a medium supplemented with 10% serum was used as a chemo-attractant in the lower chamber. Each well was freshly coated with 100 µl of Matrigel^TM (BD Bioscience) at a dilution of 1:10 in cold PBS and was then air-dried overnight before starting the

invasion assay. Cells were allowed to migrate through the membrane coated with Matrigel^{TM} at 37°C in a 5% CO_2 incubator for 24 and 48h. Non-migratory cells in the upper chamber were then gently scraped off with a cotton-tip applicator. Invading cells on the lower surface of the membrane were fixed and stained with Hematoxylin and Eosin. After staining, the total number of invading cells was counted under the light microscope (×10 objective) from 6 consecutive fields for each well**.**

H. Transwell Migration Assay

Using the transmigration chamber assay (36, 37), we assessed the cell migration ability of PLum-AD and Plum-AI cells. 8µm pore size inserts (Falcon) were placed into 24-well plates containing PrEGM in the presence or absence of 10% FBS. 2.5×10^5 cells were then loaded onto the inserts and incubated at 37°C in a humidified incubator containing 5% CO2. After 24 hrs, the inserts were removed and, using a cotton swab, the cells that didn't go through the inserts were gently scraped off. The inserts were then fixed and stained using Hematoxylin and Eosin. The membrane of the insert was then cut and mounted, on a microscopic slide, and examined under a light microscope. Cell migration was quantified by counting the number of cells that migrated through the insert (at least 5 different randomly selected fields from each insert was photographed and counted under 20x magnification).

I. RNA extraction and quantitative real time PCR (qRT-PCR)

Total RNA was extracted from PLum-AD and PLum-AI cells using the RNeasy Micro Kit (Qiagen) according to the manufacturer's instructions. cDNA was generated from total RNA using the Super Script III First Strand Synthesis System for RT-PCR (Invitrogen), and PCR was performed using Platinum Taq Polymerase (Invitrogen). For quantitative RT-PCR, the

amplification step was done using the SYBR green PCR master mix (Applied Biosystems, Bedford, MA). All reactions were run in duplicate using the specific primers listed below and all values were normalized to the house keeping gene GAPDH. The primers used were: GAPDH-F: 5' ACCTGGCTAGCGAAAAGCAA3'; GAPDH-R: 5'CCACTTTGTCAAGCTCATTTCCT3'; AR-F: GACTCTGGGAGCTCGTAAGC; AR-R: ACTCCTGGCTCAATGGCTTC; CK18-F: CTGGTCTCAGCAGATTGAGG; CK18-R: CTCCGTGAGTGTGGTCTCAG; CK14-F: GATGACTTCCGGACCAAGTT; CK14-R: TGAGGCTCTCAATCTGCATC; E-cadherin-F: GAC AACGCTCCTGTCTTCAA; E-cadherin-R: ACGGTGTACACAGCTTTCCA; Vimentin-F: AAACGAGTACCGGAGACAGG; Vimentin-R: TCTCTTCCATCTCACGCATC.

J. In Vivo Transplantation

1. *Subcutaneous Transplantation.*

A total of $1x10^6$ PLum-AD or PLum-AI cells in 50 μl was mixed 1:1 with growth factor reduced Matrigel^{TM} (Becton Dickinson) immediately prior to injection. Cells were injected subcutaneously into the flanks of 30 8-10 week old NOD-SCID male mice. 15 mice were injected with Plum-AI ,and 15 were injected with Plum-AD.All mice protocols were approved by the Institutional Animal Care and Utilization Committee (IACUC) at the American University of Beirut. All mice were housed in specific pathogen-free animal housing. Animals were sacrificed by cervical dislocation following deep anesthesia with isoflurane. Mice were euthanized upon signs of morbidity.

2. *Primary tumor studies*

Tumor size measurements were initiated upon the detection of a palpable tumor post injection. Tumor size and expansion was determined by direct physical measurements of the tumors at the primary site of injection, once per week, until the termination of the experiment.

3. *Survival experiments.*

The survival rate of mice was assessed. The overall survival is defined from the initial injection of the cells until death of mice from any cause including termination upon showing signs of morbidity. Survival curves were calculated according to Kaplan and Meier method and analyses were performed using GraphPad Prism software.

4. *Histological examination, immunohistochemistry and immunofluorescent analysis.*

Tumor type (e.g. Adenocarcinoma versus Sarcomatoid carcinoma) was assessed through histological analysis. Tumors were stained for H&E and were subjected to immunohistochemical and immunofluorescent analysis. All tumors were collected and fixed in 4% Formalin overnight, rinsed well in PBS, and transferred to 70% ethanol before standard processing to obtain paraffin-embedded sections. Unstained tissue sections were deparaffinized, and antigen retrieval was performed in a citrate buffer in a steamer at 100^0C for 60 min followed by 30 min incubation at room temperature. Slides were treated with Peroxidase block for 5 min and then blocking was performed with protein blocking buffer (NGS 10%, Triton: 0,1%,BSA: 3%, PBS) for 1hr at room temperature. Primary antibody incubation was performed overnight at 4^0C in a humidified chamber, followed by secondary biotinylated antibody block (biotinylated anti-mouse IgG and biotynilated anti-rabbit IgG, Vector laboratories) for 1h at 37°C. Slides were incubated then with

Vector ABC (Vectastain ABC Kit Peroxidase standard", Vector Laboratories) for 30 min

followed by incubation with DAB chromogen prepared in Dako DAB substrate buffer (Liquid

DAB+Substrate Chromogen system, Dako USA) for 5 min. All slides were counterstained with

hematoxylin.

Double immunofluorescence was performed on tissue sections using the same protocol

as used for IHC with the following exceptions: The secondary antibodies were Alexa Fluor 488

conjugated goat anti-mouse and goat anti-rabbit IgG and Alexa Fluor 568 conjugated goat

anti-rabbit and goat anti-mouse IgG. Slides were mounted with the anti-fade Fluoro-gel II with

Dapi. Confocal microscopic analyses were performed using Zeiss LSM 710 confocal microscope

and images were acquired and analyzed using the ZEN image software.

5. Data Analysis

Statistical analysis was performed using Microsoft Excel 2013 and plotted using

GraphPad Prism software. The significance of the data was analyzed using a Student's t-test, and

differences between two means with $p < .05$ (*) was considered significant.

RESULTS

A. Characterization of the morphology and expression profile of cultured cells derived from androgen-dependent and androgen-independent prostate cancer.

First, we sought to determine the characteristics of the newly isolated PLum-AD and PLum-AI murine PC cells in culture. Since the parental PLum cells were cultured in serum-free prostate epithelial cell basal media, PrEGM (Abou-Kheir et al, 2011), we cultured PLum-AD and PLum-AI cells with the same media. Unlike PLum-AD cells that grew in serum-free medium, PLum-AI cells grew better in 5% FBS-containing medium (Fig. 3). Both cell lines remained identical in morphology to the original tumors they were isolated from. PLum-AD cells, isolated from tumors in the presence of androgens, mainly adenocarcinoma, showed a typical epithelial morphology (cobble-stone and cell-cell interaction). PLum-AI cells, isolated from poorly differentiated/sarcomatoid carcinoma in the absence of androgen, had a typical epithelial-to-mesenchymal phenotype (migratory phenotype with minimal cell-cell interaction) (Fig.3).

PLum-AD and PLum-AI cells were stained for lineage markers including CK8, CK14 and Vimentin, which are characteristically expressed in prostate cells at different percentages. Both cell lines cells showed expression of CK8.Plum-AD cells showed a high expression of CK 14 and a low expression level of vimentin, PLum-AI cells showed the opposite where Vimentin was highly expressed and CK14 expression was almost lost (Fig. 3). These data are consistent with the morphology of the cells and also with the phenotype of the tumors they were isolated from.
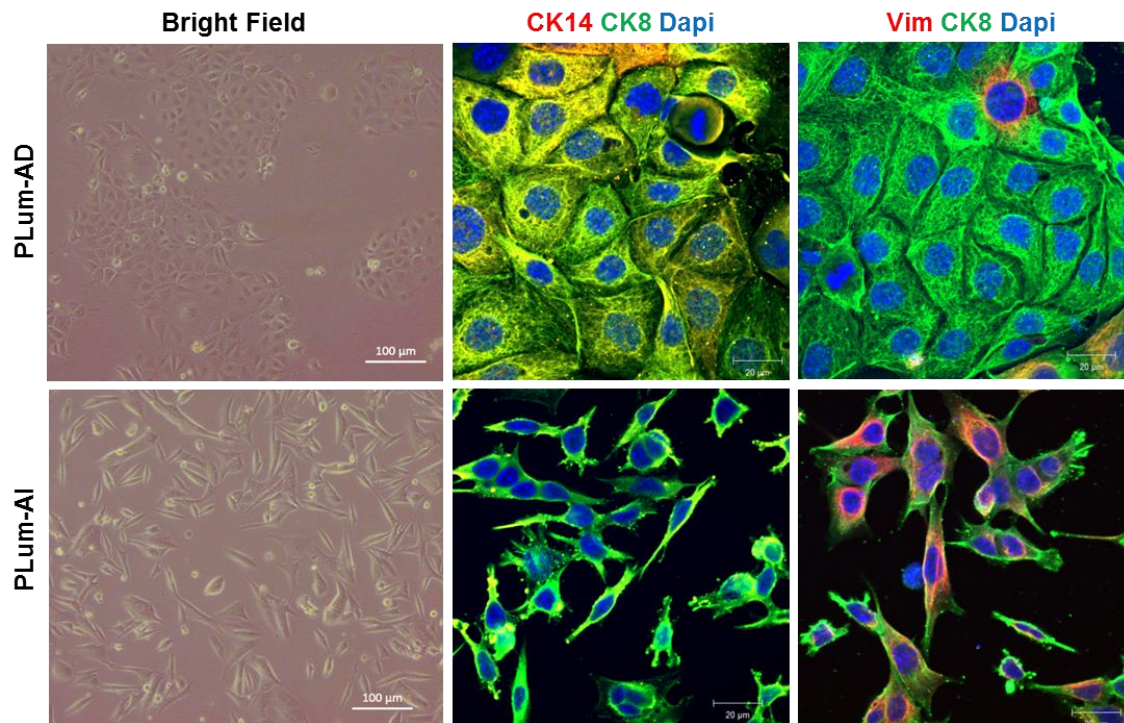
Figure 3. Morphologic and immunophenotypic characterization of PLum-AD and PLum-AI cells. Representative bright-field images (left panel) showed the typical cobble-stone epithelial phenotype of PLum-AD cells and the typical mesenchymal phenotype pf PLum-AI cells. Representative immunofluorescent images (middle and right panels) of PLum-AD and PLum-AI cells stained for the indicated antibodies and the nuclear counterstain Dapi are shown. CK14: Cytokeratin 14; CK8: Cytokeratin 8; Vim: Vimentin; Dapi: 4',6-diamidino-2-phenylindole.

To further assess and characterize the cells, a quantitative reverse transcription-PCR (qRT-PCR) and Western Blot (WB) analyses were performed (Fig. 4 and Fig. 5). To assess the effect of androgen deprivation on these established cell lines, mRNA expression levels of several genes involved in prostate lineage differentiation as well as in epithelial-to-mesenchymal transition (EMT) process were performed (Fig. 4). mRNA expression data showed higher expression in CK14 and CK8 levels in PLum-AD cells compared to PLum-AI cells. Furthermore, mRNA expression level of E-Cadherin was higher in PLum-AD compared to

PLum-AI cells while the opposite was true for vimentin expression level, consistent with the different phenotypes of the cells (Fig. 4). The expression level of AR was slightly less in PLum-AI compared to PLum-AD cells. Consistent with the mRNA expression data, PLum-AD cells showed similar results at the protein expression levels compared to PLum-AI cells confirming the epithelial phenotype of PLum-AD cells compared to the mesenchymal phenotype of PLum-AI cells (Fig. 5).
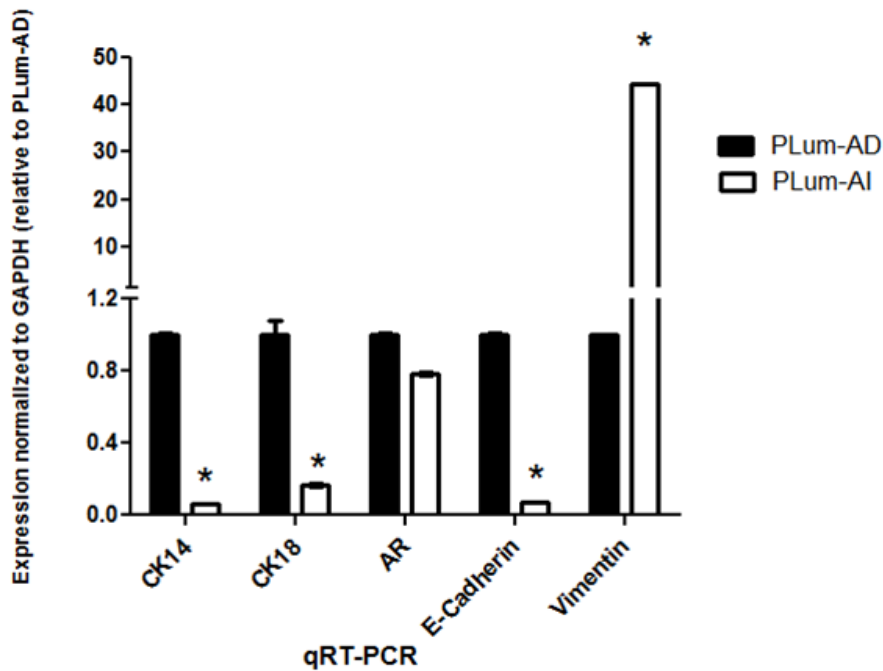

Figure 4. **Molecular characterization of PLum-AD and PLum-AI cells using qRT-PCR analysis.** The expression of different prostate epithelial lineages and mesenchymal cell markers was determined in PLum-AD and PLum-AI cells using qRT-PCR analysis. All values were normalized to GAPDH and the data were plotted relative to PLum-AD. Data represent an average of three independent experiments. The data are reported as mean ± SEM (* $P < 0.05$). AR: Androgen Receptor.
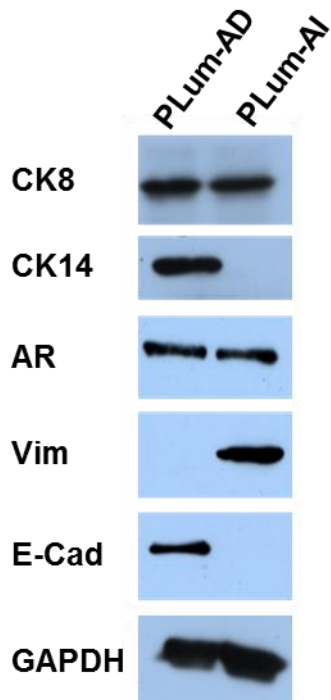
Figure 5. **Molecular characterization of PLum-AD and PLum-AI cells using WB analysis.** The expression of different prostate epithelial lineages and mesenchymal cell markers was determined in PLum-AD and PLum-AI cells using WB analysis. A representative image of three independent experiments. E-Cad: E-Cadherin; GAPDH: Glyceraldehyde 3-phosphate dehydrogenase.

B. Evaluation of stem/progenitor cell activity in PLum-AD and PLum-AI cells (Self-renewal and differentiation)

Sphere-formation assay (Abou-Kheir et al, 2010; Abou-Kheir et al, 2011) was performed on the cells to assess whether or not they possess stem/progenitor cell properties. Both cell lines formed 3-D protospheres (prostate spheres) when kept in serum-free PrEGM media and suspended in a semi-solid ECM like Matrigel[TM] at a concentration of 2000 cells/well. While PLum-AI cells formed stellate spheres supporting their mesenchymal phenotype, PLum-AD cells formed large regular spheres reflecting their epithelial nature (Fig. 6). This shows the presence of a population of cells that expresses stem cell characteristics.
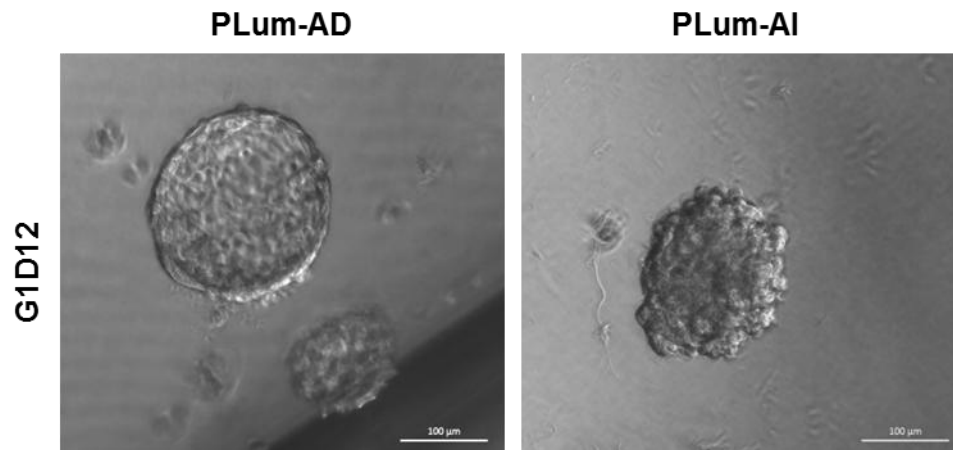

Figure 6. Sphere-forming ability of PLum-AD and PLum-AI cells. Representative bright-field images of PLum-AD and PLum-AI prostate spheres (protospheres) in Matrigel[TM] at G1D12 (Generation 1/ Day 12) are shown. A representative image of two independent experiments

To assess the self-renewal abilities, a property of stem/progenitor cells, of these cell lines, spheres formed were further propagated for 6 generations. Sphere forming units (SFUs) were calculated for each generation (Fig. 7). This was done by dividing the number of spheres counted by the number of input cell. This reveals that both cell lines have a population of stem/progenitor cells with self-renewal ability maintained throughout propagation.

Spheres from both cell lines were stained for F-actin, CK14, CK8 and b3 Tubulin to assess the differentiation abilities of the two cell lines (Fig. 8). F-actin staining revealed the architectural organization of the spheres, where PLum-AD spheres showed intact organization while PLum-AI spheres showed disorganized phenotype. Both PLum-AD and PLum-AI spheres showed differentiation potential since they stained positive for CK14 (less in PLum-AI), CK8 and b3-Tubulin.
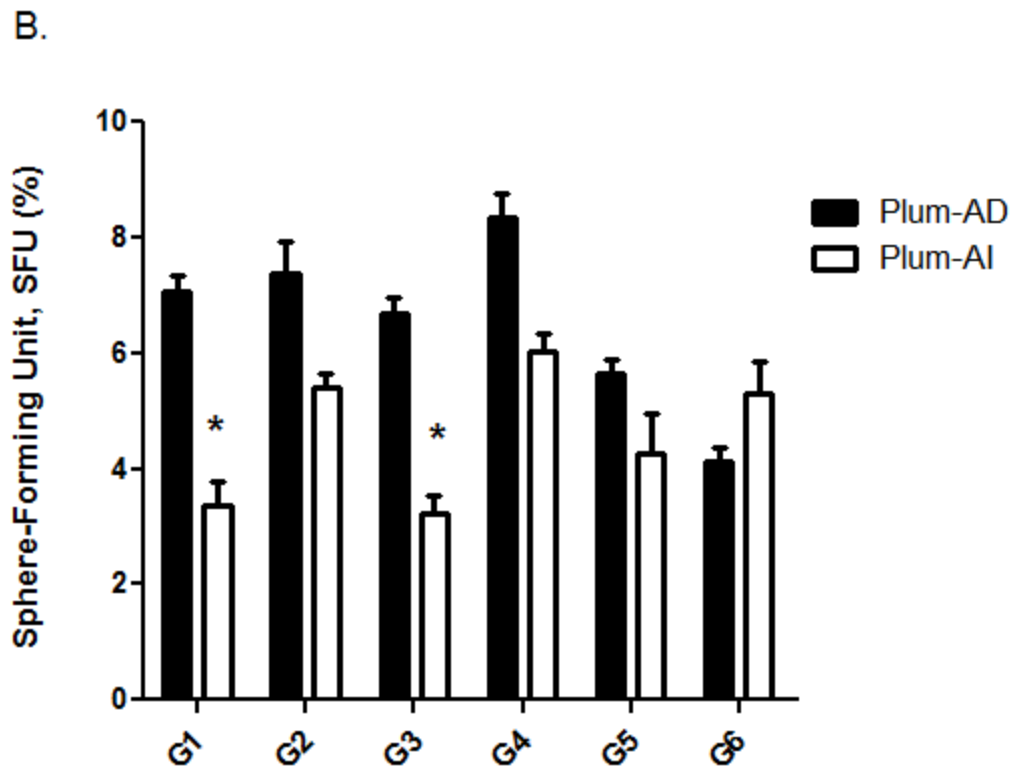
B.

Figure 7. Self-renewal ability of PLum-AD and PLum-AI cells. PLum-AD and PLum-AI cells were plated in Matrigel^TM at a density of 2,000 cells/well in a 12-well plate for sphere formation assay. Sphere forming units expressed as % of 2,000 input cells at each generation obtained from serially passaged protospheres are shown. Data represent an average of two independent experiments. The data are reported as mean ± SEM (* $P < 0.05$).
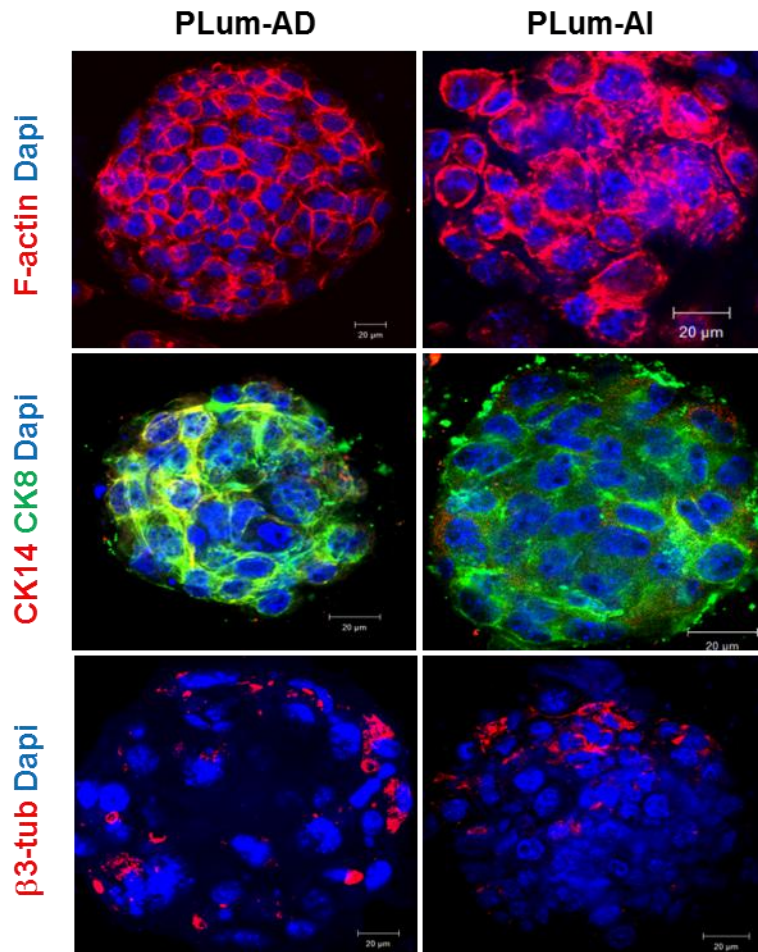
Figure 8. Differentiation potential of PLum-AD and PLum-AI cells. Immunofluorescent images of confocal cross sections from representative PLum-AD and PLum-AI protospheres stained for F-actin, CK14, CK8, b3 tubulin and Dapi are shown.

C. Assessing the cell migration and invasion potential of PLum-AD and PLum-AI cells.

      To assess the cell migration ability of PLum-AD and PLum-AI cells, cell migration assay was performed using the transwell migration assay in the presence or absence of the chemoattractant FBS (Fig. 9). Migration in both cell lines was low in the absence of FBS with Plum-AI cells showing a considerably higher migratory potential than PLum-AD cells. PLum-AI seems to have a more aggressive nature than PLum-AD even in the absence of the chemoattractant. However, in the presence of FBS, the cell lines showed a noticeably higher cell migration and a much higher migratory potential in PLum-AI than in PLum-AD cells. This is consistent with the results obtained previously showing that PLum-AI cells possess a mesenchymal phenotype which makes them more aggressive than the epithelial PLum-AD cells.
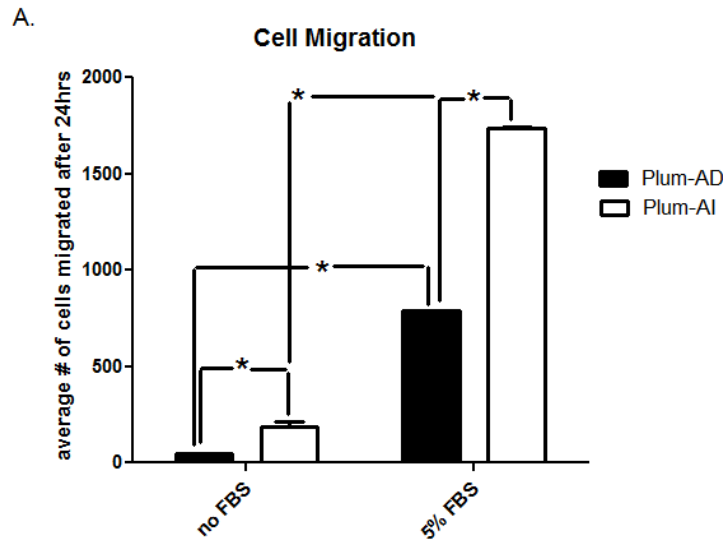

Figure 9. **Migration potential of PLum-AD and PLum-AI cells.** The cell migration potential in response to FBS was assessed in PLum-AD and PLum-AI cells using the transwell-migration assay. Data represent an average of three independent experiments. The data are reported as mean ± SEM (* P < 0.05).

To evaluate the cell invasion ability of PLum-AD and PLum-AI cells, cell invasion was performed using the transwell invasion assay in the presence or absence of the chemoattractant FBS (Fig. 10). Similar to the cell migration assay, and consistent with the aggressiveness of the cell line and its EMT phenotype, PLum-AI showed a significantly higher invasion potential as compared to PLum-AD under both conditions. This suggests that PLum-AI is much more invasive and aggressive than PLum-AD.
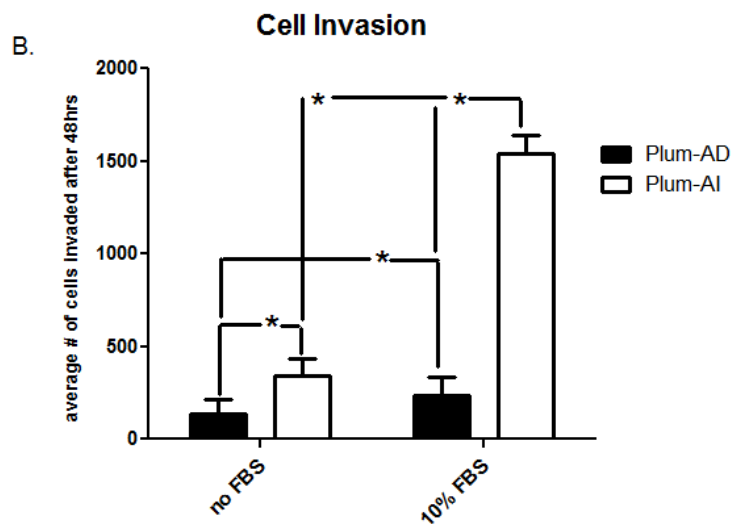

Figure 10. **Invasion potential of PLum-AD and PLum-AI cells.** The cell invasion potential in response to FBS was assessed in PLum-AD and PLum-AI cells using the transwell-invasion assay. Data represent an average of three independent experiments. The data are reported as mean ± SEM (* $P < 0.05$).

D. **Assessing the tumorigenic potential of PLum-AD and PLum-AI**

To characterize the tumorigenic properties of PLum-AD and PLum-AI, cells from both cell lines were injected into the flanks of 30 8-10 week old NOD-SCID mice subcutaneously. Tumor size was measured once every week upon its detection until time of death (Fig. 11). Mice that were injected with PLum-AI cells developed a tumor in less than half the time that was needed for those injected with PLum-AD to develop a tumor. Not to mention that the tumors formed by PLum-AI cells were significantly larger in volume than those formed by PLum-AD cells suggesting the more aggressive nature of PLum-AI cells.
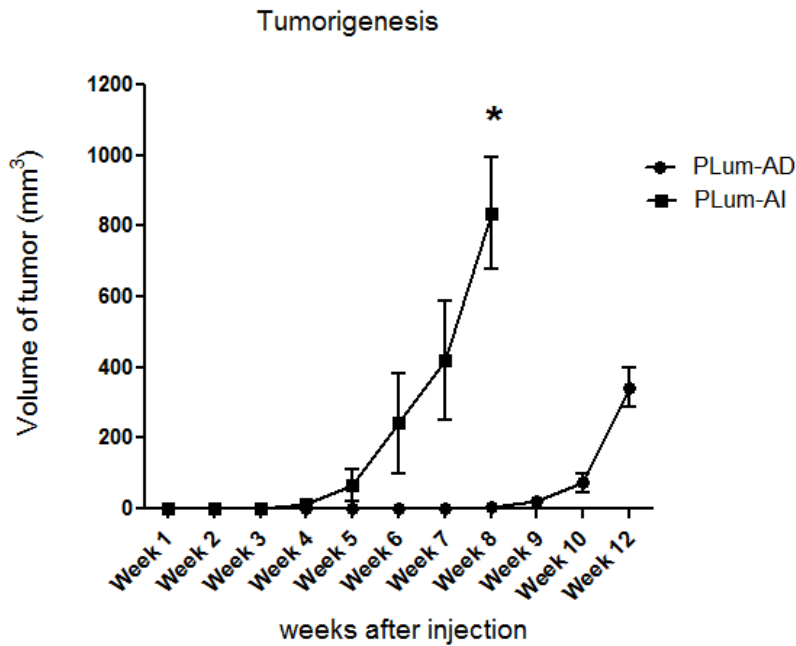
Figure 11. **Tumorigenic potential of PLum-AD and PLum-AI cells.** 1×10^6 PLum-AD and PLum-AI cells were subcutaneously transplanted in 8-10 weeks-old NOD-SCID mice. Tumor size measurements were initiated upon the detection of a palpable tumor post injection. Tumor size and expansion were determined by direct physical measurements of the tumors at the primary site of injection, once per week, until the termination of the experiment. Data represent an average of n=3 mice. The data are reported as mean ± SEM (* $P<0.05$).

In addition, the survival rate of mice from time of injection till death from any cause was documented (Fig. 12). Mice that were injected with PLum-AD cells showed a delay in death by three weeks compared to those injected with PLum-AI cells, suggesting further the aggressiveness of PLum-AI cells.
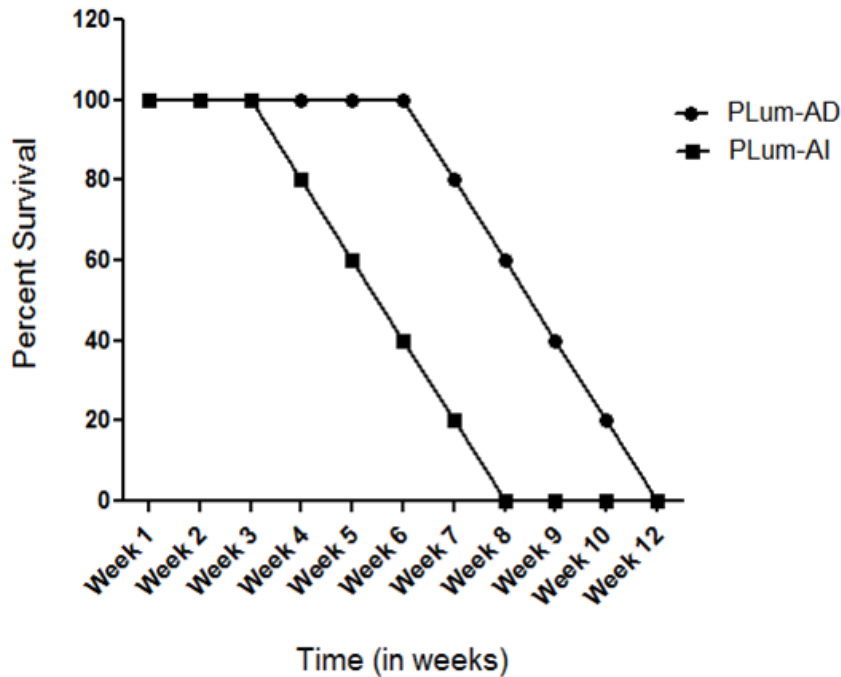

Figure 12. **Survival analysis.** The survival curves of 30 NOD-SCID mice injected subcutaneously with 1×10^{6} PLum-AD and PLum-AI cells were generated. P<0.05.

Upon histological examination of PLum-AD and PLum-AI tumors by H&E, our data revealed that the tumors generated remained faithful to the phenotype of the cells in vitro. Hence, Plum-AD cells generated mostly adenocarcinoma with minor patches of sarcomatoid carcinoma, while Plum-AI cells generated mostly sarcomatoid carcinomas (Fig. 13). Serial sections of the primary mass of the tumors were obtained and subjected to immunohistochemistry and immunofluorescence analysis to study the type and cell composition of the tumors. Our data revealed that the adenocarcinoma tumors formed by PLum-AD cells showed high expression of

AR. On the contrary, sarcomatoid carcinomas formed by PLum-AI cells showed a low expression for AR (Fig. 13). This is consistent with the tumor phenotypes where adenocarcinomas typically express AR while sarcomatoid carcinomas lose the AR expression. Further immunofluorescent analysis revealed that tumors formed by PLum-AD cells expressed CK8, a marker of luminal cells and some cells expressed CK14, a marker for basal cells. In addition, cells co-expressing CK8/CK14 were also detected (Fig. 14). This is consistent of the glandular phenotype of adenocarcinomas. Tumors generated by PLum-AI cells also showed CK8 and CK14 expression (Fig. 14). Interestingly, vimentin expression, a marker of epithelial-to-mesenchymal transition, was more prominent in tumors generated by Plum-AI cells compared to Plum-AD cells (Fig. 14). This is consistent with the nature of the two tumors and it correlates with the hypothesis that PLum-AI cells might represent the CRPC stage of the disease.
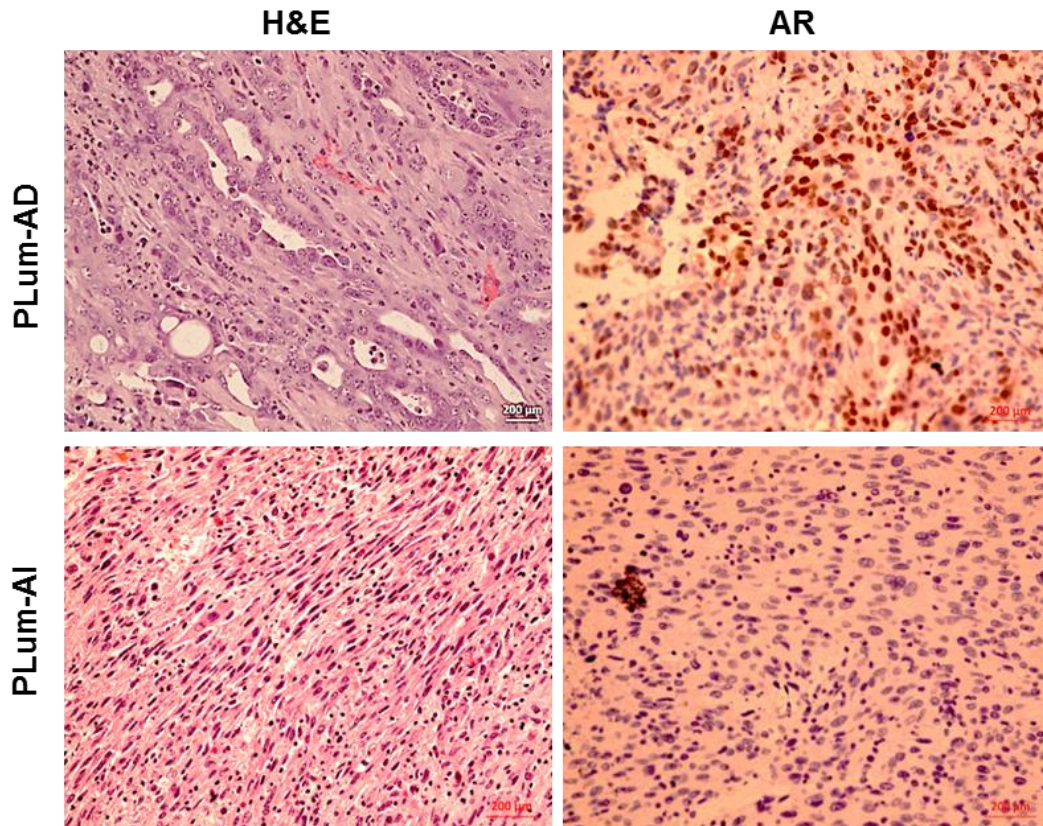
Figure 13. **Characterization of subcutaneously transplanted tumors initiated from PLum-AD and PLum-AI cells.** Cross-sections of subcutaneous tumors stained with H&E (left panel) showed typical adenocarcinoma in PLum-AD tumors and sarcomatoid carcinoma in PLum-AI tumors. Immunohistochemical analysis of AR (right panel) showed high expression in PLum-AD tumors and low expression in PLum-AI tumors.

Figure 14. **Immunofluorescent analysis of PLum-AD and PLum-AI tumors.** Cross-sections of PLum-AD and PLum-AI subcutaneous tumors were stained with CK14, CK8, vimentin and Dapi.

E. Proliferation of PLum-AI and PLum-AD in response to Bicalutamide and Metformin

Cell proliferation of PLum-AD and PLum-AI cells, in the absence or presence of Bicalutamide (10 μM), was assayed using th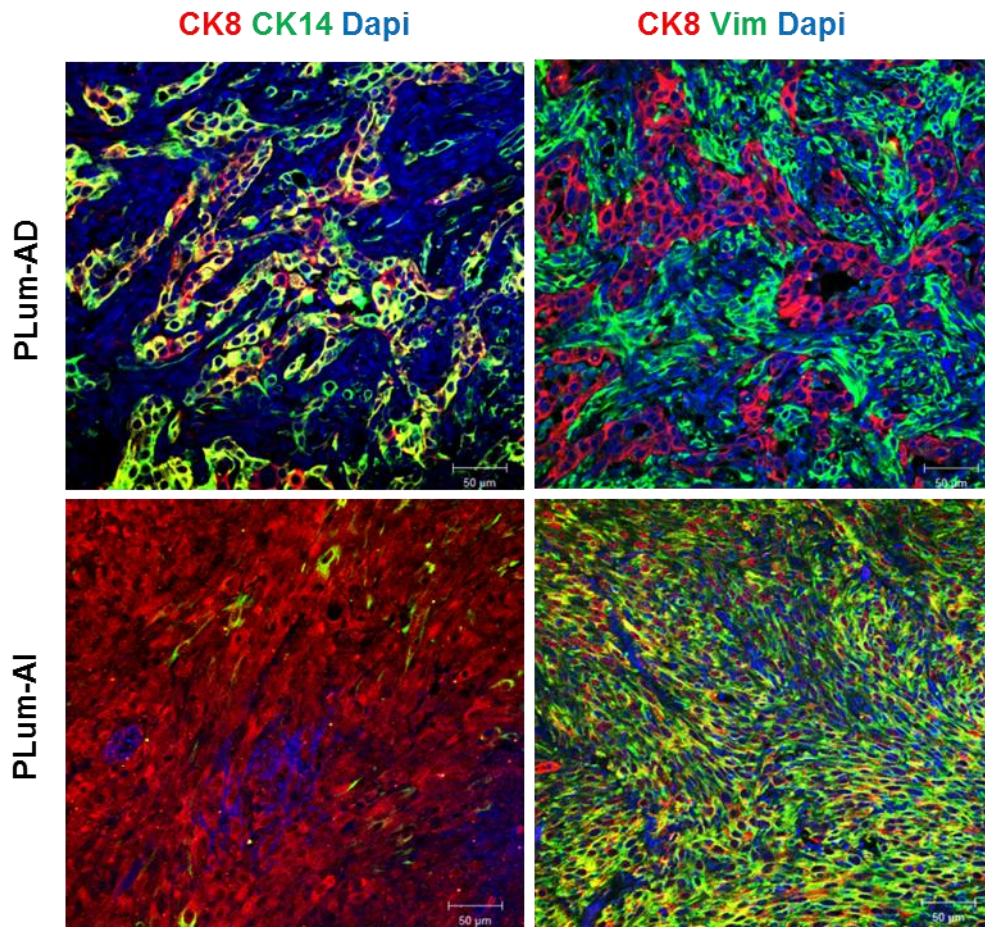e MTT assay (Fig. 15A). Cells were seeded in 96-well plates in triplicate in PrEGM media. The next day, cells were treated with either Vehicle (DMSO) or Bicalutamide (10 μM). After 72 hrs, the MTT dye reaction was read using a spectrophotometer (Fig. 15A). Interestingly, PLum-AD cells showed a decrease in cell viability when treated with Bicalutamide, while no effect was observed on PLum-AI cells. The fact that the androgen receptor antagonist Bicalutamide had no effect on PLum-AI cell viability goes in parallel with our hypothesis that those cells might model castration-resistant prostate cancer (CRPC) where the latter becomes non-responsive to androgen receptor antagonist treatments. Unlike PLum-AI cells, PLum-AD cells were responsive to Bicalutamide and therefore the cells might model tumors that are responsive to anti-androgen treatments. Interestingly, Metformin, a standard anti-diabetic drug with potential anti-neoplastic effects, inhibited PLum-AD and PLum-AI cell proliferation in a dose-dependent manner (Fig. 15B). This stands as a proof of principle for using the new cell model system to screen for new therapeutics that might affect CRPC. Further experiments with different drugs need to be used to confirm our results.
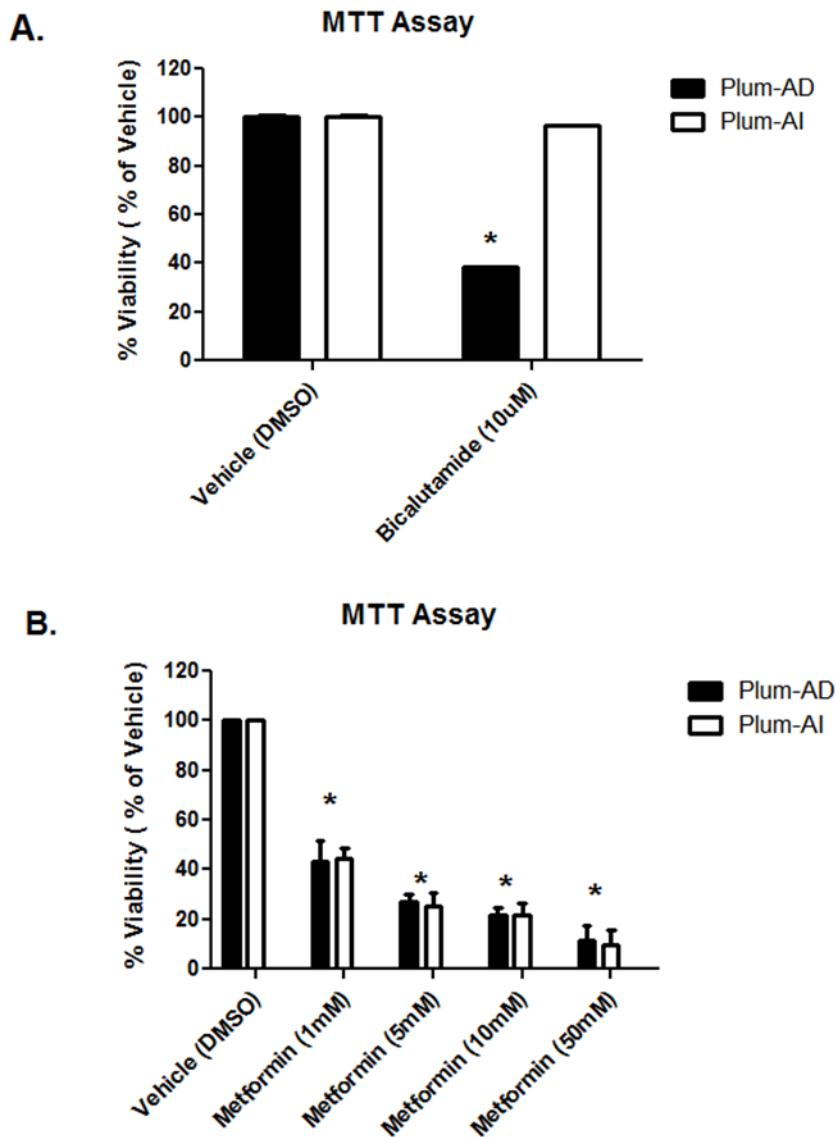
Figure 15. **Assessing the proliferative index of PLum-AD and PLum-AI cells in response to different drugs.** The cell viability index of PLum-AD and PLum-AI cells in response to Bicalutamide **(A)** or Metformin **(B)** treatment using MTT assay was assayed for 72 hrs. Data represent an average of three independent experiments. The data are reported as mean ± SEM (* $P < 0.05$).

DISCUSSION

Significant progress has been achieved in understanding the mechanisms underlying the advancement of prostate cancer (Shalken et al, 2015). Most patients respond initially to androgen deprivation therapy but eventually relapse, develop resistance and metastasize entering the castration-resistant phase of the disease (Suzuki et al, 2003). EMT is a process that has been implicated in cancer metastasis (Sun et al, 2011). EMT usually occurs only during embryonic development; however research has shown that it is reactivated in cases of malignancies (Cottard et al, 2013). This transformation has been shown to be responsible for formation of metastatic prostate cancer and its spread into other tissue sites (Suzuki et al, 2015). This process has also been shown to confirm cancer stem cell properties (Mani et al, 2008). Cell lines representing the progression of prostate cancer from its early androgen-dependent state to its late castration-resistant state are few (Abou kheir et al, 2011). This study aimed at identifying the functional differences and mechanisms underlying the progression of prostate cancer from the androgen-dependent stage (PLum-AD) to the castration-resistant or androgen-independent stage (PLum-AI).

To characterize the morphology and to study the functional properties of cultured cells derived from androgen-dependent and androgen-independent prostate cancer, cells were cultured in PrEGM media. Both cell lines were successfully propagated each under its own conditions. Not only did these cells grow successfully, they also maintained the morphology of the tumors they were respectively isolated from. PLum-AD cells, isolated from tumors in the presence of androgens, mainly adenocarcinoma, showed a typical epithelial glandular morphology which is characteristic of prostate adenocarcimona. PLum-AI cells, isolated from sarcomatoid carcinoma in the absence of androgen, had a typical epithelial-to-mesenchymal elongated fibroblastic

phenotype. Further immunofluorscent staining against the epithelial lineage marker CK14 and the mesenchymal marker vimentin was done to confirm the previous conclusions. It has been suggested that EMT is a characteristic of cancer cells during their metastasis from a primary organ to other secondary organs (Jones et al, 2011). In this process, epithelial cell layers lose polarity and cell-cell interaction. These cells acquire expression of mesenchymal components and manifest a migratory phenotype (Soltermann et al, 2008). To evaluate the effect of androgen deprivation on mRNA expression levels of several genes involved in EMT process, qRT-PCR was performed. As a feature of aggressive tumors, epithelial to mesenchymal transition (EMT) is characterized by reduced E-cadherin and increased N-cadherin expression (Kang et al, 2004, Gravdal et al, 2007). This was confirmed by measuring the mRNA expression level of E-Cadherin in PLum-AD compared to PLum-AI cells. PLum-AI cells showed high expression of the mesenchymal marker N-cadherin, while PLum-AD showed epithelial marker expression suggesting the presence of an epithelial to mesenchymal transition as the disease moves forward. Western blot results further proved this transformation showing the up-regulation of vimentin and down-regulation of E-cadherin in PLum-AI cells as compared to Plum-AD cells. In carcinoma cells, this is referred to as fibroblast-like transformation and is the classic example of EMT observed in sarcomatoid carcinomas (Soltermann et al, 2008). The above data shows that the cell lines. PLum-AD and PLum-AI may be used to recapitulate the transition of prostate adenocarcinoma into CRPC.

In the field of cancer biology, cancer stem cells have been defined functionally by two major criteria: their ability to undergo self-renewal and their ability to produce differentiated progeny (Wang et al, 2013). Previous studies have shown murine prostate cells are able to grow in Matrigel and form prostate spheres (Xin et al, 2007). These sphere-forming cells have the

ability to self-renew and are capable of multilineage differentiation (Xin et al, 2007) .The presence of prostate cancer stem-like cells in PLum-AD and PLum-AI was confirmed and evaluated by using the sphere-formation assay. These spheres were able to further self-renew and to maintain their sphere forming ability. Not to mention that the expression of the different epithelial lineage markers (CK8, CK14 and b3 tubulin) by those sphere-forming cells showed there capability of multilineage differention. These cells appear to be highly tumorigenic and may be the cells that drive tumor formation and mediate tumor metastasis(Tang et al, 2006). The above demonstrates the self-renewal and differentiation capacity of prostate stem cells in both PLum-AD and PLum-AI.

During the EMT process, epithelial cells acquire a migratory and invasive mesenchymal phenotype (Sun et al, 2011). This was obvious when migration and invasion assays were performed on PLum-AD and PLum-AI to assess their migration and invasion potential. As expected, PLum-AI, being the aggressive form of the disease and reflecting the CRPC phase, showed significantly higher migratory and invasion capabilities.

Cells from both cell lines PLum-AD and PLum-AI were injected into 7 week old NOD-SCID mice subcutaneously. Tumor development was much faster, more potent and more fatal in mice injected with PLum-AI cells than those injected with PLum-AD cells. This, in addition to their EMT phenotype in vitro, shows that PLum-AI cell line represents the advanced and more aggressive form of prostate cancer. H&E staining on PLum-AD derived tumors showed a glandular epithelial morphology in keeping with adenocarcinoma., while those on PLum-AI derived tumors showed elongated cells consistent with a sarcomatoid carcinoma.

When stained against AR, the tumors derived from PLum-AD cells maintained high expression of AR. However tumors derived from PLum-AI cells showed less expression of AR.

During androgen-independent progression, prostate cancer cells develop a variety of cellular pathways to survive in an androgen-depleted environment (Pienta et al, 2006). While our results showed that AR is scarce in PLum-AI cells, other studies showed that there exists an over expression of AR in cases of CRPC (Chen et al, 2004). It is believed that the AR signaling pathway remains implicated throughout all the stages of prostate cancer and the reactivation of AR is thought to be the key driver of CRPC progression (Shalken et al, 2015, Knudsen et al, 2011). Raised levels of AR has also been detected in CRPC tissue specimens (Watson et al, 2010). Despite the discrepancies in research when it comes to AR signaling in prostate cancer, many believe that the AR signaling pathway is one of the main target pathways to be studied when speaking of a therapeutic approach. Nevertheless, AR-independent targets and approaches are also under investigation.

Tumor tissue sections were stained with CK8, CK14 and vimentin. The high expression of vimentin by PLum-AI cells was suggestive of an epithelial to mesenchymal transformation indicating a much higher degree of metastasis in PLum-AI than in PLum-AD levels. This is correlated with the hypothesis that PLum-AI cells might represent the CRPC stage of the disease. Recent research has shown the link between androgen deprivation and high vimentin levels which are associated with cancer metastasis (Sun et al, 2011). This confirms the high tumorigenic and metastatic profile of the PLum-AI cells as compared to PLum-AD mimicking CRPC.

Bicalutamide is a drug that works by blocking androgen receptors. Bicalutamide binds to androgen receptors, prevents their activation and accelerates their degradation (Furr et al, 1996). This drug is used for the treatment of the earlier stages of prostate cancer. Most advanced prostate cancer become resistant to Bicalutamide (Balk et al, 2002).That been said, MTT was

done on both PLum-AI and PLum-AD cells to assess cell proliferation under the effect of bicalutamide. Bicalutamide inhibited cell proliferation of PLum-AD, but had no effect on PLum-AI cells. Our data shows consistency with what is already known about the effect of the anti-androgen bicalutamide on human prostate cancer. This further illustrates how the PLum-AI and PLum-AD cell model tackles the progression of prostate cancer from its early stages to its advanced stages.

Metformin is a widely used anti-diabetic drug. It is most commonly used in the treatment of type 2 diabetes, gestational diabetes, polycystic ovarian syndrome and obesity (Dowling et al, 2011). Metformin activates the AMPK pathway, a major energy sensor in the cell, which is proposed as a promising therapeutic target in cancer nowadays (Ben Sahra et al, 2010). It has been shown that metformin treatment is associated with a decrease in cancer risk (Christos et al, 2012). Not only does metformin seem to have a preventive cancer effect , there is increasing evidence of a potential efficacy of this drug as a new anticancer agent (Ben Sahra et al, 2010). Metformin has been shown to display anti-tumoral properties in human prostate cancer cell lines and animal models (Dirat et al, 2014). In nude mice, metformin was shown to reduce the formation of prostate cancer metastasis. Metformin also impedes cell motility in PC3 and DU145 prostate cancer cells (Dirat et al, 2014). In an attempt to see the effect of metformin on prostate cancer cell proliferation, MTT was performed on PLum-AD and PLum-AI cells. Different concentrations of metformin (1Mm, 5mM, 10Mm and 50mM) were used to treat the cells. Both experiments showed that Metformin significantly inhibited the proliferation of both cell lines, even at a low metformin concentration of 1 mM. This provides promising data that metformin may be useful in treating prostate cancer even at its advanced resistant stages. More research

needs to be done to further confirm the possibility of metformin as a new potential therapeutic target.

These data suggest that the newly isolated cell lines represent a new in vitro model of androgen-dependent and –independent prostate cancer where they recapitulate the progression of the disease to a more invasive phenotype upon androgen deprivation. More work has to be done to decipher the molecular mechanisms involved in this progression that would eventually lead us to new therapeutic targets. Such study will likely lead to a comprehensive understanding of the mechanisms exploited by the cancer and eventually new therapeutic targets could be recognized that might help improve managing, or even curing, the disease.

REFERENCES

Abou-Kheir WG, Hynes PG, Martin PL, Pierce R, Kelly K."Characterizing the contribution of stem/progenitor cells to tumorigenesis in the Pten-/-TP53-/- prostate cancer model". Stem Cells 28(2010): 2129–2140

Abou-Kheir, Wassim, et al. "Self-renewing Pten-/-TP53-/-protospheres produce metastatic adenocarcinoma cell lines with multipotent progenitor activity." *PloS one* 6.10 (2011): e26112.

Ahmed, M., et al. "Transurethral microwave thermotherapy (Prostatron version 2.5) compared with transurethral resection of the prostate for the treatment of benign prostatic hyperplasia: a randomized, controlled, parallel study." *British journal of urology* 79.2 (1997): 181-185.

Attard G, Belldegrun AS, de Bono JS. "Selective blockade of androgenic steroid synthesis by novel lyase inhibitors as a therapeutic strategy for treating metastatic prostate cancer". *BJU Int.* 96.9(2005): 1241–6.

Balk, Steven P. "Androgen receptor as a target in androgen-independent prostate cancer." *Urology* 60.3 (2002): 132-138.

Balk SP, Ko YJ, Bubley GJ . "Biology of prostate-specific antigen". *J. Clin. Oncol.* **21** .2(2003): 383–91

Bonkhoff, Helmut, Ute Stein, and Klaus Remberger. "The proliferative function of basal cells in the normal and hyperplastic human prostate." *The Prostate* 24.3 (1994): 114-118.

Bonkhoff, Helmut, and Klaus Remberger. "Differentiation pathways and histogenetic aspects of normal and abnormal prostatic growth: a stem cell model." *The Prostate* 28.2 (1996): 98-106.

Bostwick, David G. "Prostatic intraepithelial neoplasia." *Current urology reports* 1.1 (2000): 65-70.

Chen, Charlie D., et al. "Molecular determinants of resistance to antiandrogen therapy." *Nature medicine* 10.1 (2004): 33-39.

Cottard, Félicie, et al. "Constitutively active androgen receptor variants upregulate expression of mesenchymal markers in prostate cancer cells." *PloS one* 8.5 (2013): e63466.

DeMarzo, Angelo M., et al. "Pathological and molecular aspects of prostate cancer." *The Lancet* 361.9361 (2003): 955-964.

Di Lorenzo, Giuseppe, et al. "Castration-resistant prostate cancer." *Drugs* 70.8 (2010): 983-1000.

Dirat, Beatrice, et al. "Inhibition of the GTPase Rac1 mediates the anti-migratory effects of metformin in prostate cancer cells." *Molecular cancer therapeutics* (2014): molcanther-0102.

Dowling, Ryan JO, Pamela J. Goodwin, and Vuk Stambolic. "Understanding the benefit of metformin use in cancer treatment." *BMC medicine* 9.1 (2011): 33.

Furr, B. J. "The development of Casodex (bicalutamide): preclinical studies." *European urology* 29 (1995): 83-95.

Gelmann, Edward P. "Molecular biology of the androgen receptor." *Journal of Clinical Oncology* 20.13 (2002): 3001-3015.

Gonzales, C., et al. "Effect of red maca (Lepidium meyenii) on prostate zinc levels in rats with testosterone-induced prostatic hyperplasia." *Andrologia* 44.s1 (2012): 362-369.

Gravdal, Karsten, et al. "A switch from E-cadherin to N-cadherin expression indicates epithelial to mesenchymal transition and is of strong and independent importance for the progress of prostate cancer." *Clinical Cancer Research* 13.23 (2007): 7003-7011.

Heinlein, Cynthia A., and Chawnshang Chang. "Androgen receptor in prostate cancer." *Endocrine reviews* 25.2 (2004): 276-308.

Herschman JD, Smith DS, Catalona WJ . "Effect of ejaculation on serum total and free prostate-specific antigen concentrations". *Urology* **50** .2(1997): 239–43

Hong, Hao, et al. "Positron emission tomography imaging of prostate cancer." *Amino acids* 39.1 (2009): 11-27.

Horoszewicz, Julius S., et al. "LNCaP model of human prostatic carcinoma." *Cancer research* 43.4 (1983): 1809-1818.

Isaacs, John T., and Donald S. Coffey. "Etiology and disease process of benign prostatic hyperplasia." *The Prostate* 15.S2 (1989): 33-50.

Jones, Anna C., et al. "Early growth response 1 and fatty acid synthase expression is altered in tumor adjacent prostate tissue and indicates field cancerization." *The Prostate* 72.11 (2012): 1159-1170.

Kaighn, M. E., et al. "Establishment and characterization of a human prostatic carcinoma cell line (PC-3)." *Investigative urology* 17.1 (1979): 16-23.

Kang, Yibin, and Joan Massagué. "Epithelial-mesenchymal transitions: twist in development and metastasis." *Cell* 118.3 (2004): 277-279.

Klotz, L. "Combined androgen blockade in prostate cancer: meta‐analyses and associated issues." *BJU international* 87.9 (2006): 806-813.

Knudsen, Karen E., and William Kevin Kelly. "Outsmarting androgen receptor: creative approaches for targeting aberrant androgen signaling in advanced prostate cancer." (2011): 483-493.

Lalani, E-N., A. Stubbs, and G. W. H. Stamp. "Prostate cancer; the interface between pathology and basic scientific research." *Seminars in cancer biology*. Vol. 8. No. 1. Academic Press, 1997.

Long, Ronan M., et al. "Prostate epithelial cell differentiation and its relevance to the understanding of prostate cancer therapies." *Clinical Science* 108.1 (2005): 1-12.

Mani, Sendurai A., et al. "The epithelial-mesenchymal transition generates cells with properties of stem cells." *Cell* 133.4 (2008): 704-715.

McNicholas, Consultant Neurological Surgeon Tom, and Roger Kirby. "Benign prostatic hyperplasia and male lower urinary tract symptoms (LUTS)." *Clinical evidence* 2011 (2011).

Montalvo, L., et al. "Effect of flutamide-induced androgen-receptor blockade on adenylate cyclase activation through G-protein coupled receptors in rat prostate." *Cellular signalling* 12.5 (2000): 311-316.

Myers, Robert P (2000). "Structure of the adult prostate from a clinician's standpoint". *Clinical Anatomy* **13**.3(2000) : 214–5.

Perlmutter, Mark A., and Herbert Lepor. "Androgen deprivation therapy in the treatment of advanced prostate cancer." *Reviews in urology* 9.Suppl 1 (2007): S3.

Pienta, Kenneth J., and Deborah Bradley. "Mechanisms underlying the development of androgen-independent prostate cancer." *Clinical Cancer Research* 12.6 (2006): 1665-1671.

Princivalle, Marc, et al. "Rapid suppression of plasma testosterone levels and tumor growth in the dunning rat model treated with degarelix, a new gonadotropin-releasing hormone antagonist." *Journal of Pharmacology and Experimental Therapeutics* 320.3 (2007): 1113-1118.

Pulukuri, Sai Murali Krishna, and Jasti S. Rao. "Activation of p53/p21Waf1/Cip1 pathway by 5-aza-2'-deoxycytidine inhibits cell proliferation, induces pro-apoptotic genes and mitogen-activated protein kinases in human prostate cancer cells." *International journal of oncology* 26.4 (2005): 863-871.

Rizos, Christos V., and Moses S. Elisaf. "Metformin and cancer." *European journal of pharmacology* 705.1 (2013): 96-108.

Sahra, Issam Ben, et al. "Metformin in cancer therapy: a new perspective for an old antidiabetic drug?." *Molecular cancer therapeutics* 9.5 (2010): 1092-1099.

Schalken, Jack, and John M. Fitzpatrick. "Enzalutamide: Targeting the androgen signalling pathway in metastatic castration-resistant prostate cancer." *BJU international* (2015).

Shelley, Mike, et al. "Chemotherapy for hormone-refractory prostate cancer." *The Cochrane Library* (2006).

Shen, Michael M., and Cory Abate-Shen. "Molecular genetics of prostate cancer: new prospects for old challenges." *Genes & development* 24.18 (2010): 1967-2000.

Soltermann, Alex, et al. "Prognostic significance of epithelial-mesenchymal and mesenchymal-epithelial transition protein expression in non–small cell lung cancer." *Clinical Cancer Research* 14.22 (2008): 7430-7437.

Stone, Kenneth R., et al. "Isolation of a human prostate carcinoma cell line (DU 145)." *International journal of cancer* 21.3 (1978): 274-281.

Sun, Yuting, et al. "Androgen deprivation causes epithelial–mesenchymal transition in the prostate: implications for androgen-deprivation therapy." *Cancer research* 72.2 (2012): 527-536.

Suzuki, H., et al. "Androgen receptor involvement in the progression of prostate cancer." *Endocrine-related cancer* 10.2 (2003): 209-216.

Tang, Dean G., et al. "Prostate cancer stem/progenitor cells: identification, characterization, and implications." *Molecular carcinogenesis* 46.1 (2007): 1-14.

Wang, Yue J., et al. "Sphere-forming assays for assessment of benign and malignant pancreatic stem cells." *Pancreatic Cancer*. Humana Press, 2013. 281-290.

Watson, Philip A., et al. "Constitutively active androgen receptor splice variants expressed in castration-resistant prostate cancer require full-length androgen receptor." *Proceedings of the national academy of sciences* 107.39 (2010): 16759-16765.

Wellington, K; Keam, S. J. "Bicalutamide 150mg: A review of its use in the treatment of locally advanced prostate cancer". *Drugs* 66.6(2006): 837–50.

Xin, Li, et al. "Self-Renewal and Multilineage Differentiation In Vitro from Murine Prostate Stem Cells." *Stem Cells* 25.11 (2007): 2760-2769.